Synthetic Metals 201 (2015) 43–48

Contents lists available at ScienceDirect

Synthetic Metals

journal homepage: www.elsevier.com/locate/synmet

Naphtho[4,3,2,1-*lmn*][2,9]phenanthrolines: Synthesis, characterization, optical properties and light-induced electron transfer in composites with the semiconducting polymer MEH-PPV

Denis S. Baranov [a,b], Alexandr G. Popov [a,b], Mikhail N. Uvarov [a,*], Maxim S. Kazantsev [b,c], Evgeny A. Mostovich [b,c], Evgeni M. Glebov [a,b], Leonid V. Kulik [a,b]

[a] V.V. Voevodsky Institute of Chemical Kinetics and Combustion, Siberian Branch of the Russian Academy of Science, 630090 Novosibirsk, Russian Federation
[b] Novosibirsk State University, 630090 Novosibirsk, Russian Federation
[c] N.N. Vorozhtsov Novosibirsk Institute of Organic Chemistry, Siberian Branch of the Russian Academy of Science, 630090 Novosibirsk, Russian Federation

ARTICLE INFO

Article history:
Received 20 October 2014
Received in revised form 12 January 2015
Accepted 13 January 2015
Available online xxx

Keywords:
Diazapyrenes
Synthesis
Spectroscopy
Light-induced electron transfer

ABSTRACT

Novel naphtho[4,3,2,1-*lmn*][2,9]phenanthrolines were synthesized via reaction between 1,5-diethynyl-9,10-anthraquinones and urea in DMF. Their HOMO and LUMO levels determined from optical spectroscopy and cyclic voltammetry are in good agreement with those determined from quantum chemical calculation. Light-induced electron transfer from the semiconducting polymer MEH-PPV to the synthesized molecules was detected by EPR-spectroscopy, showing their possible applicability as electron acceptors in bulk heterojunction organic solar cells. The synthesized naphtho[4,3,2,1-*lmn*][2,9]phenanthrolines can be used as building blocks for larger molecules with an extended π-conjugated system, which can be used as acceptors in organic photovoltaics.

1. Introduction

In organic photovoltaics, considerable attention is devoted to solar cells with a bulk heterojunction structure where fullerenes are used as a semiconducting acceptor component [1]. Owing to the success of these devices, the fullerenes are prominent amongst a small series of acceptor materials suitable for organic solar cells [2]. Nevertheless, the search for effective acceptor materials is progressing rapidly and molecules of novel types are coming to view [3]. There is potential in an alternative approach based on the application of simpler and cheaper acceptor materials with small molecules [4,5]. The number of tested substances is constantly growing, however their variety is limited and represented mostly by perylene derivatives [6,7]. Simultaneously a large number of similar polycondensed systems remain unexplored. Of particular interest are the polycyclic heteroaromatic compounds containing either heteroatoms or acceptor substitutes and the hybrid molecules that combine the conjugated acceptor and donor parts [8]. The special significance of polycyclic arenes (pyrene, perylene, coronene) for organic electronics [9] makes the analysis of similar heteroaromatic systems interesting. Additionally, the insertion of nitrogen atoms into polycondensed system enhances resistance to degradation [10]. Therefore, we have paid attention to the development and study of new, polycondensed diazahetarenes, the analogues of perylene [11] and benzopyrene.

2. Experimental

2.1. Synthesis

2.1.1. Copper(I) acetylides (general procedure) (**1**)

A mixture of CuCl (2.5 g, 0.025 mol), NH_4Cl (5.3 g, 0.1 mol), $NH_2OH{\cdot}HCl$ (0.7 g, 0.01 mol), 25% aqueous NH_3 (13 ml) in 100 ml H_2O was stirred at room temperature under argon atmosphere. After stirring for 20 min, alkyne (0.02 mol) was added into the mixture over a period of 1 h. After stirring the reaction mixture for a further 4 h, the yellow precipitate copper acetylide was filtered, washed with EtOH, and dried in vacuum.

2.1.2. 1,4-Diiodo-9,10-anthraquinone (**2**)

1,4-Diamino-9,10-anthraquinone (2.4 g, 0.01 mol) was suspended in a mixture of AcOH (55 ml) and H_2SO_4 (10 ml). Nitrosylsulfuric acid (2 g $NaNO_2$, 20 ml H_2SO_4) was added over 30 min. After the mixture had been stirred for 30 min, the dark solids were filtered. The filtrate was added in portions in a mixture of KI (6 g, 0.036 mol) and AcOH (50 ml) at 50–60 °C. Then the

* Corresponding author. Tel.: +7 383 333 22 97; fax: +7 383 330 73 50.
E-mail address: uvarov@kinetics.nsc.ru (M.N. Uvarov).

http://dx.doi.org/10.1016/j.synthmet.2015.01.012
0379-6779/

mixture had stirred at 70 °C for 3 h. The brown precipitates were filtered, then washed with H_2O and $NaHSO_3$ solution. The crude product was purified by column chromatography on SiO_2 (elution with toluene). Yield 2.4 g (52%), mp 219–220 °C (toluene) (lit. mp 218–219 °C [12]).

*2.1.3. Synthesis of 1,4-bis(R-ethynyl)-9,10-anthraquinones (general procedure) (**3**)*

A mixture of 1,4-diiodo-9,10-anthraquinone (1.1 mmol) and copper acetylides (2.5 mmol) in 15 ml of pyridine was stirred under stream of argon at 60–65 °C for 0.5 h. Then ethyl acetate (100 ml) was added, the organic layers were washed with 5% aqueous NH_3 (50 ml) and water (100 ml), dried over $MgSO_4$. The crude product was purified by column chromatography on SiO_2 (elution with toluene). Subsequent recrystallization gave pure compounds **3**.

*2.1.3.1. 1,4-Bis(3-prop-2-yloxypropyn-1-yl)-9,10-anthraquinone (**3a**).* Yield 180 mg (41%), mp 97–98 °C (petroleum ether). ^{1}H NMR ($CDCl_3$, 400 MHz) δ: 1.28 (d, 12H, 4Me, *J* 6.0 Hz), 4.04 (m, 2H, $2CHMe_2$), 4.56 (s, 4H, $2CH_2$), 7.78 (m, 4H, H_{Ar}), 8.27 (m, 2H, H_{Ar}). ^{13}C NMR ($CDCl_3$, 100 MHz) δ: 22.10 (4Me), 56.57 ($2CHMe_2$), 71.06 ($2CH_2$), 85.12, 94.82 (2C≡CC), 123.24, 127.24, 133.42, 134.19, 134.62, 139.17 (C_{Ar}), 181.95 (2C=O). IR (ν/cm^{-1}): 2853, 2895, 2927, 2966, 2980 (CH_2OCHMe_2), 2204 (C≡C), 1674 (C=O). Found (%): C, 78.08; H, 5.80. Calc. for $C_{26}H_{24}O_4$ (%): C, 77.98; H, 6.04.

*2.1.3.2. 1,4-Bis(octyn-1-yl)-9,10-anthraquinone (**3b**).* Yield 260 mg (56%), mp 78–79 °C (petroleum ether). ^{1}H NMR ($CDCl_3$, 400 MHz) δ: 0.92 (t, 6H, 2Me, *J* 7.0 Hz), 1.37 (m, 8H, $2(CH_2)_2$), 1.54 (m, 4H, $2CH_2$), 1.72 (m, 4H, $2CH_2$), 2.60 (t, 4H, $2CH_2$Pr, *J* 7.2 Hz), 7.71 (s, 2H, $2H_{Ar}$), 7.76 (m, 2H, $2H_{Ar}$), 8.27 (m, 2H, $2H_{Ar}$). ^{13}C NMR ($CDCl_3$, 100 MHz) δ: 14.24, 20.42, 22.74, 28.77, 28.89, 31.56 (2Hex), 80.73, 99.75 (2C≡C), 124.00, 127.16, 133.66, 133.94, 134.46, 139.34 (C_{Ar}), 182.33 (2C=O). IR (ν/cm^{-1}): 2854, 2926, 2951 (Hex), 2216 (C≡C), 1676 (C=O). Found (%): C, 85.37; H, 7.49. Calc. for $C_{30}H_{32}O_2$ (%): C, 84.87; H, 7.60.

*2.1.4. Synthesis of 2,7-DiR-naphtho[4,3,2,1-lmn][2,9]phenanthroline (general procedure) (**4**)*

Method A: a mixture 1,4-bis(R-ethynyl)-9,10-anthraquinone (0.4 mmol), urea 4 g (66.7 mmol) in 2.8 ml of DMF was boiled for 0.5–3 h. A mixture of toluene (50 ml) and water (50 ml) was then added, the organic layer was separated, dried over $MgSO_4$ and evaporated to dryness under reduced pressure. The crude product was purified by column chromatography on SiO_2 (elution with toluene). Subsequent recrystallization gave pure compounds **4**.

*2.1.4.1. 2,7-Bis(prop-2-yloxymethyl) naphtho[4,3,2,1-lmn][2,9] phenanthroline (**4a**).* Yield 70 mg (43%), mp 104–105 °C (petroleum ether). ^{1}H NMR ($CDCl_3$, 400 MHz) δ: 1.39 (d, 12H, 4Me, *J* 6.0 Hz), 3.96 (m, 2H, $2CHMe_2$), 5.51 (s, 4H, $2CH_2$), 7.90 (m, 2H, H_{Ar}), 8.17 (s, 2H, $2H_{Ar}$), 8.22 (s, 2H, $2H_{Ar}$), 9.44 (m, 2H, H_{Ar}). ^{13}C NMR ($CDCl_3$, 100 MHz) δ: 22.49 (4Me), 71.96 ($2CH_2$), 72.22 ($2CHMe_2$), 116.65, 117.13, 125.07, 129.45, 130.32, 132.93, 136.44, 146.51, 156.83 (C_{Ar}). Found (%): C, 78.40; H, 6.51; N, 6.97. Calc. for $C_{26}H_{26}N_2O_2$ (%): C, 78.36; H, 6.58; N, 7.03.

*2.1.4.2. 2,7-Dihexylnaphtho[4,3,2,1-lmn][2,9]phenanthroline (**4b**).* Yield 60 mg (35%), mp 81–83 °C (petroleum ether). ^{1}H NMR ($CDCl_3$, 400 MHz) δ: 0.91 (t, 6H, 2Me, *J* 7.1 Hz), 1.39 (m, 8H, 2 $(CH_2)_2$), 1.51 (m, 4H, $2CH_2$), 2.04 (m, 4H, $2CH_2$), 3.26 (t, 4H, $2CH_2$Pr, *J* 7.7 Hz), 7.84 (s, 2H, H_{Ar}), 7.90 (m, 2H, H_{Ar}), 8.06 (m, 2H, H_{Ar}), 9.50 (m, 2H, H_{Ar}). ^{13}C NMR ($CDCl_3$, 100 MHz) δ: 14.29, 22.82, 29.41, 30.45, 32.00, 39.31 (Hex), 116.35, 118.10, 125.09, 129.23, 129.84, 133.09, 136.09, 146.54, 159.65 (C_{Ar}). HMRS, *m*/*z*: 422.2719 (calc. for $C_{30}H_{34}N_2$: 422.2717[M]$^+$).

Method B: a mixture of 1,4-diiodo-9,10-anthraquinone (1.1 mmol) and copper acetylides (2.5 mmol) in 15 ml of pyridine was stirred under a stream of argon at 60–65 °C for 0.5 h. Then ethyl acetate (100 ml) was added, the organic layers were washed with 5% aqueous NH_3 (50 ml) and water (100 ml), dried over $MgSO_4$ and evaporated to dryness under reduced pressure. Further 10 g urea and 7 ml DMF was added, the mixture was boiled for 0.5 h. Isolation and purification of compounds **4** analogous to the method A.

*2.1.4.3. 2,7-Bis(prop-2-yloxymethyl) naphtho[4,3,2,1-lmn][2,9] phenanthroline (**4a**).* Yield 130 mg (30%), mp 104–105 °C (petroleum ether).

*2.1.4.4. 2,7-Bis(benzyloxymethyl) naphtho[4,3,2,1-lmn][2,9] phenanthroline (**4c**).* Yield 130 mg (24%), mp 154–155 °C (toluene–petroleum ether). ^{1}H NMR ($CDCl_3$, 400 MHz) δ: 4.86 (s, 4H, $2CH_2Ph$), 5.20 (s, 4H, $2CH_2O$), 7.35 (t, 2H, $H_{p\text{-}Ph}$, *J* 7.5 Hz), 7.42 (m, 4H, $2H_{o\text{-}Ph}$), 7.52 (m, 4H, $H_{m\text{-}Ph}$), 7.90 (m, 2H, H_{Ar}), 8.18 (s, 2H, H_{Ar}), 8.25 (s, 2H, H_{Ar}), 9.44 (m, 2H, H_{Ar}). ^{13}C NMR ($CDCl_3$, 100 MHz) δ: 73.30, 73.98 (CH_2OCH_2), 116.82, 117.18, 125.11 (C_{Ar}), 127.99 ($C_{p\text{-}Ph}$), 128.08, 128.69 ($C_{o\text{-}Ph}$ and $C_{m\text{-}Ph}$), 129.56, 130.38, 132.91, 136.50 (C_{Ar}), 138.29 ($C_{i\text{-}Ph}$), 146.68, 155.96 (C_{Ar}). Found (%): C, 82.82; H, 5.22; N, 5.45. Calc. for $C_{34}H_{26}N_2O_2$ (%): C, 82.57; H, 5.30; N, 5.66.

*2.1.4.5. 2,7-Diphenylnaphtho[4,3,2,1-lmn][2,9]phenanthroline (**4d**).* Yield 135 mg (30%), mp 265–266 °C (toluene). ^{1}H NMR

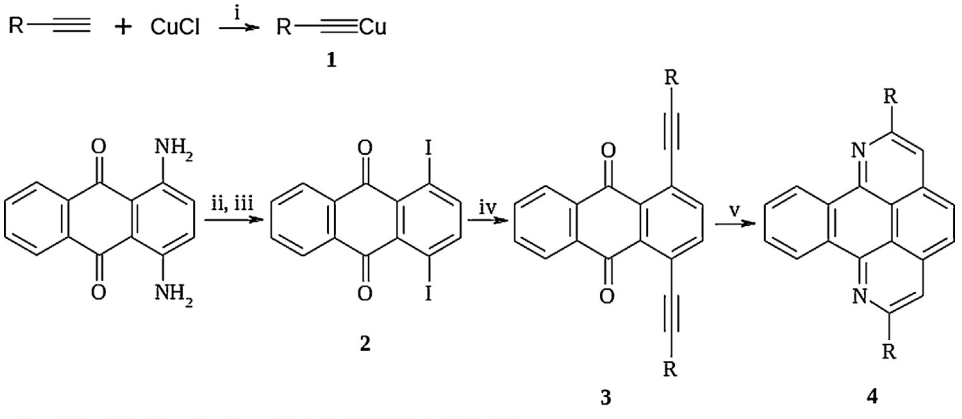

Scheme 1. *Reagents and conditions*: (i), NH_4Cl, NH_3, $NH_2OH{\cdot}HCl$, H_2O, r.t., 5 h; (ii), $NaNO_2$, H_2SO_4, AcOH, r.t., 1 h; (iii), KI, AcOH, 70 °C, 3 h; (iv), RC≡CCCu, Py, 75 °C, 0.5 h; and (v), $(NH_2)_2CO$, DMF, reflux, 0.5 h.

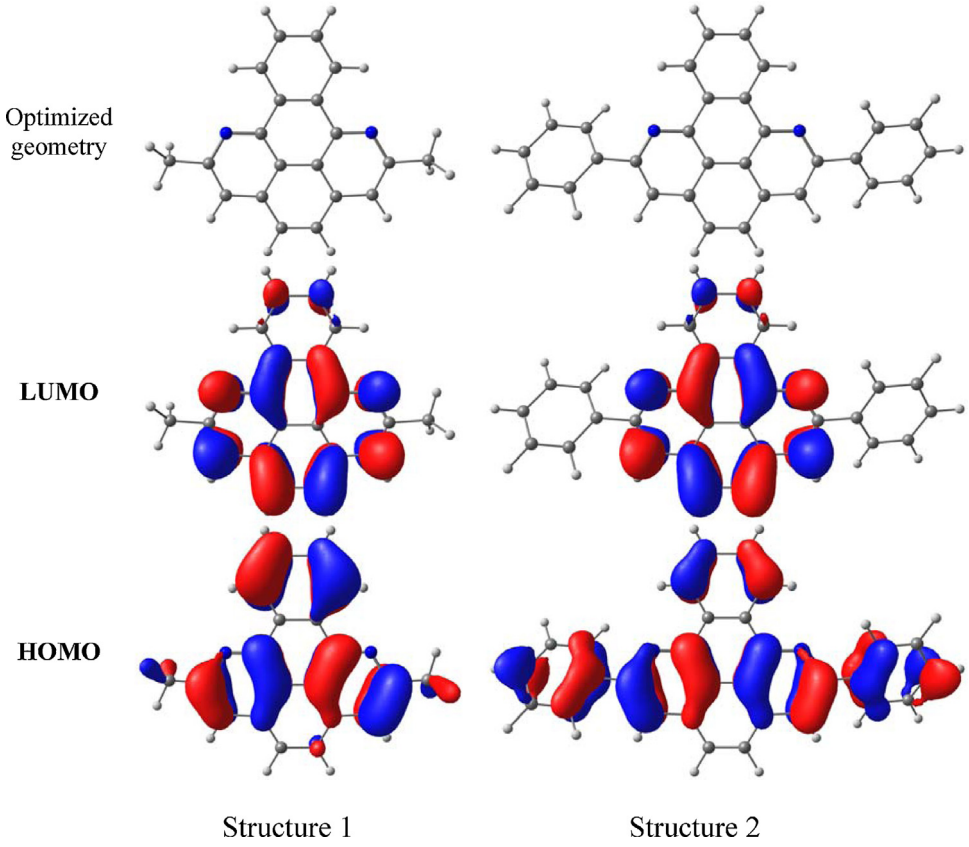

Fig. 1. The optimized geometry and the electronic density contours, calculated at DFT B3LYP/def2-TZVP level, for the HOMO and LUMO contour isovalue 0.03.

($CDCl_3$, 400 MHz) δ: 7.53 (m, 2H, $H_{p\text{-Ph}}$), 7.63 (m, 4H, $H_{m\text{-Ph}}$), 7.95 (m, 2H, H_{Ar}), 8.16 (s, 2H, H_{Ar}), 8.41 (s, 2H, H_{Ar}), 8.47 (m, 4H, $H_{o\text{-Ph}}$), 9.60 (m, 2H, H_{Ar}). ^{13}C NMR ($CDCl_3$, 100 MHz) δ: 115.95, 117.04, 125.36 (C_{Ar}), 127.80, 129.11 ($C_{o\text{-Ph}}$ and $C_{m\text{-Ph}}$), 129.28, 129.59, 130.50, 133.36, 136.76 (C_{Ar}), 140.12 ($C_{i\text{-Ph}}$), 147.07, 154.20 (C_{Ar}). Found (%): C, 88.74; H, 4.48; N, 6.86. Calc. for $C_{30}H_{18}N_2$ (%): C, 88.64; H, 4.46; N, 6.89.

2.2. General

Combustion analysis was performed with a CHN-analyzer (Model 1106, 'Carlo Erba', Italy). The NMR spectra were recorded on a Bruker AV 400 spectrometer (400.13 MHz) in $CDCl_3$. Melting points were determined with a Kofler apparatus. Mass spectra were obtained on a Thermo Electron Corporation DFS mass spectrometer (70 eV), using direct injection, the temperature of the ionization chamber was 220–270 °C. IR-spectra were recorded in KBr pellets on a 'Bruker Vector 22' instrument. Cyclic voltammetry (CVA) measurements were carried out in CH_2Cl_2 solution on a computer controlled P-8nano potentiostat/galvanostat (Elins, Russia) in combination with three-electrode cell (Gamry), 0.1 M tetrabytylammonium hexafluorophosphate being used as supporting electrolyte. The Pt, Pt wire and Ag/AgCl were used as working, counter and reference electrode, respectively. The reference electrode was calibrated by measuring the redox potential of ferrocene.

Column chromatography was performed on 60 (Merck) and the Silufol UV-254 plates were used for TLC analysis. All reagents were purchased from commercial sources.

All DFT calculations were performed using the Siberian Supercomputing Center [13]. For preliminary geometry optimization *semi-empirical* AM1 from MOPAC2012 was used [14]. The final geometry optimization step was done with ORCA 3.0.1 package by DFT B3LYP def2-TZVP or 6-31G(d) basis [15]. All visualizations were done using Gabedit 2.4.8 software [16].

The UV–vis absorption spectra were recorded using an Agilent 8453 spectrophotometer (Agilent Technologies). Luminescence spectra were recorded with a FLSP-920 spectrofluorimeter ("Edinburgh Instruments") with excitation wavelength 336 nm. Typically, toluene was used as a solvent, and the typical concentrations of investigated substances were about 10^{-5} M. Extinction coefficients ε were determined at maximum absorption in visible light region. Photoluminescence quantum yield φ values were derived using the anthracene ethanol solution as well known standard ($\varphi_{anthr} = 0.27$) [17]. Thin films of **4a–d** were obtained by spin coating from toluene solution onto glass substrate.

EPR spectra were obtained using an X-band ELEXSYS ESP-580 EPR spectrometer equipped with a cavity (Bruker SHQEW) at room temperature, mw frequency 9.8488 GHz, mw power 6.3 mW, modulation amplitude 3 G. To prepare an EPR sample chlorobenzene solution of **4d** and MEH-PPV (Aldrich) was prepared at 1:2 weight ratio in the tube with 4.5 mm inner diameter, and chlorobenzene was evaporated. At EPR cavity, the sample was illuminated by visible light of incandescent lamp, light power irradiating the sample was about 0.1 W.

3. Results and discussion

3.1. Synthesis and characterization

A general path of the synthesis of polycondensed heterocycles is shown in Scheme 1. The starting compounds necessary for producing target acetylene substrates were obtained as shown in Scheme 1. The corresponding copper acetylides were produced in the usual way from alkynes and CuCl in aqueous solutions of NH_3, NH_4Cl, and $NH_2OH{\cdot}HCl$ with yield 80–90%. Diiodide was

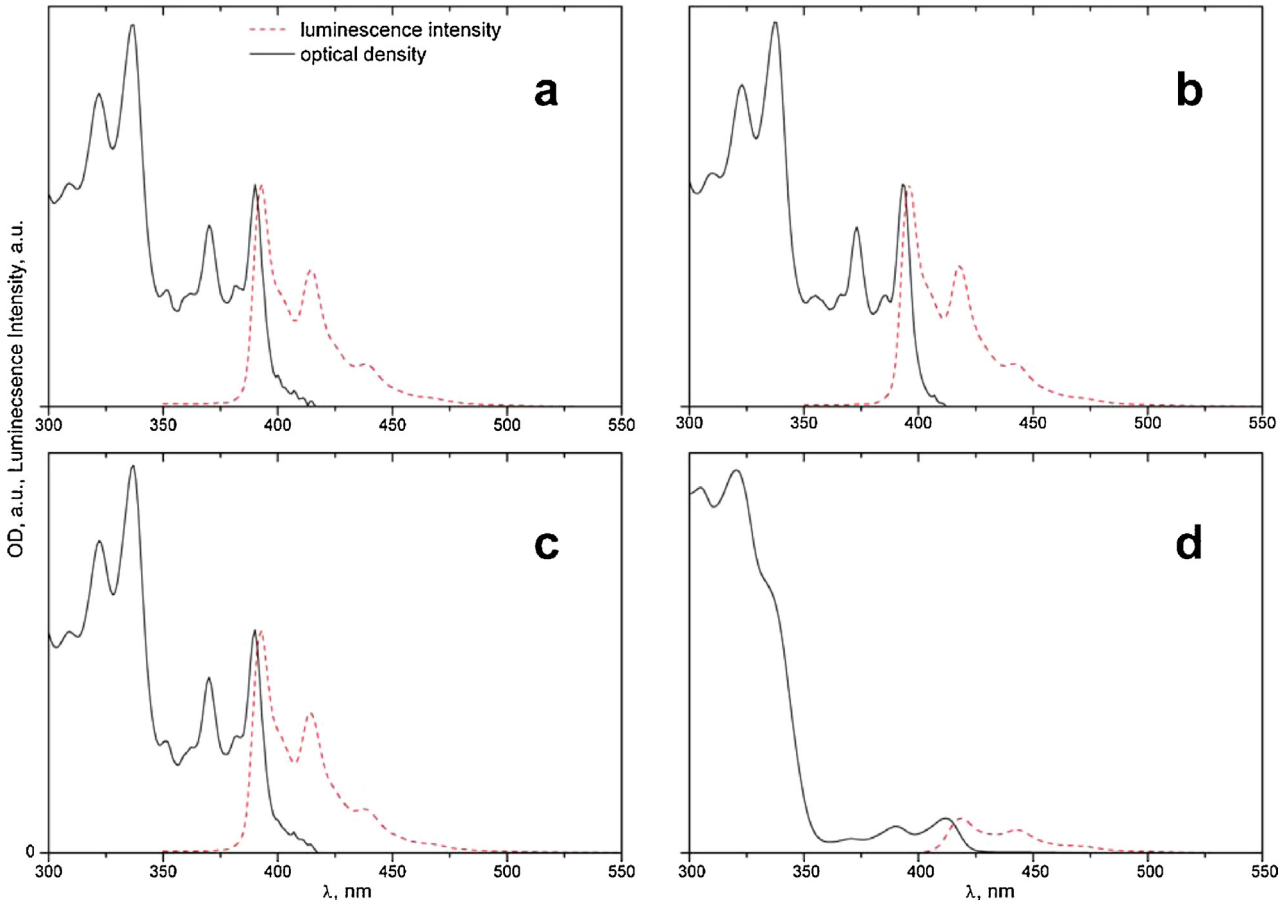

Fig. 2. UV–vis absorption spectra (solid lines) and luminescence emission spectra (dashed lines) of **4a–d** in toluene solution.

Table 1
Oxidation potentials, HOMO and LUMO energy levels, the HOMO–LUMO gap, the characteristic extinction coefficients ε and the luminescence quantum yield for the φ compounds **4a–d**.

Compound	E_{Ox},V (vs. Fc/Fc$^+$)	E_{Red}, V (vs. Fc/Fc$^+$)	HOMO (eV)[a,b]	LUMO (eV)[a,b]	HOMO–LUMO (eV)[a,b]	LUMO (eV)[c]	HOMO–LUMO(eV)[c]	ε, 10^3 M^{-1} cm^{-1} (λ, nm)	φ
4a	1.07	−2.13	−5.59[a]/−6.19[b]	−2.83[a]/−2.26[b]	2.76[a]/3.93[b]	−2.43	3.16	14 (390)	0.2
4b	1.09	−2.21	−5.55[a]/−6.19[b]	−2.85[a]/−2.26[b]	2.70[a]/3.93[b]	−2.42	3.13	13 (393)	0.13
4c	1.02	−2.02	−5.46[a]/−6.19[b]	−2.63[a]/−2.26[b]	2.83[a]/3.93[b]	−2.30	3.16	13 (390)	0.34
4d	1.12	−2.35	−5.78[a]/−6.02[b]	−2.97[a]/−2.36[b]	2.97[a]/3.66[b]	−2.81	2.97	3.3 (412)	0.14

[a] HOMO and LUMO was derived by a comparison of onset oxidation potential with the ionization potential of ferrocene.
[b] HOMO, LUMO and HOMO–LUMO gap were estimated from quantum chemical calculations.
[c] LUMO was calculated from the electrochemical HOMO and HOMO–LUMO optical gap derived from the intersection point of absorption spectrum and luminescence emission spectrum.

synthesized by diazotization with nitrosylsulfuric acid in AcOH diamine with subsequent substitution of diazonium groups by iodine in AcOH with KI with yield 52%. For the preparation of 1,4-bis(R-ethynyl)-9,10-anthraquinones we have found that the Castro method is convenient [18]. The final product was produced using two modifications of the reaction of heterocycle annelation (methods A and B). In the former case (the method A), the prepared alkyne was boiled with excess $(NH_2)_2CO$ in DMF for 0.5 h. However, the low stability of the alkyne during the isolation and purification has a negative effect on the final yield of heterocycles. In the method B, to optimize the process, the two last transformations (cross-coupling and heterocyclization) were carried out in an one-pot without alkyne purification and isolation. The latter method appeared to be more rational. The compounds were characterized by elemental analysis, IR, ^{1}H NMR, ^{13}C NMR and mass spectrometry.

3.2. Theoretical calculations

To get detailed information on structural aspects and electronic distribution in synthesized molecules quantum chemical calculations were performed by using DFT B3LYP hybrid functional and dev2-TVZP basis set [19,20]. For optimization step the atom-pairwise dispersion correction with the Becke–Johnson damping scheme (D3BJ) [21,22] was utilized.

Quantum chemical calculations were performed for two structures. The Structure 1 had the methyl groups substituents (the substance **4** with R = Me). The Structure 1 represented molecules **4a–c** since negligible effect of such displacement on electronic density distribution was expected. This replacement allowed to avoid numerous conformational isomers of alkyl chains in **4a–c**. The Structure 2 corresponded to **4d** without any replacement.

The optimized geometries and the electronic density distributions of HOMO and LUMO for the Structures 1 and 2 are depicted in Fig. 1. The dihedral angles between the phenyl rings and condensed aromatic core were calculated from the geometrically optimized structure of the molecule. It was found that the phenyl rings were slightly twisted and dihedral angles were equal $\theta = 23.1^{\circ}$. The main difference between these Structures was that the HOMO density was located on the condensed aromatic core for the Structure 1 while it was partially expanded on phenyl rings for the Structure 2. However, LUMO is concentrated only on the aromatic core for both structures. The calculated HOMO levels are −5.84 eV and −5.64 eV for the Structures 1 and 2, respectively. The calculated LUMO levels were −1.87 eV and −1.97 eV for the Structures 1 and 2, respectively. The HOMO–LUMO gap was 0.1 eV smaller for the Structure 2, which was probably caused by larger electron density delocalization.

3.3. Spectroscopic and electrochemical properties

UV–vis absorption spectra and luminescence spectra of **4a–c** in solution had the same shape and differed from the spectra of **4d** (see Fig. 2). According to the insight from quantum chemical calculation the phenyl rings in **4d** affect the electronic properties. From the intersection point of absorption spectrum and normalized luminescence emission spectrum the HOMO–LUMO gap was obtained and presented in Table 1.

Fig. 3 shows UV–vis absorption spectra of thin solid films of **4b** and **d**. The spectra of **4a** and **c** were nearly identical to that of **4b**. Slight red shift (about 10 nm) of the absorption spectra was observed both for solid films of **4b** and **d**, as compared to their solution spectra. This was explained by aggregation and enhanced π–π interactions between the polycondensed heterocycle cores. This effect is similar to the well-known red-shift of the absorption spectra of conjugated polymers upon crystallization [23].

To evaluate the HOMO and LUMO energy levels, cyclic voltammetry (CVA) in combination with optical spectroscopy was employed. The cyclic voltammetry revealed irreversible oxidation and quasi-reversible reduction peaks for compounds **4a–d** (Fig. 4). The HOMO and LUMO energy levels were estimated using onset oxidation and reduction potentials in the cyclic voltammogram according to Eqs. (1) and (2):

$$E_{\mathrm{HOMO}} = -e(E_{\mathrm{Ox}}^{\mathrm{onset}} - E_{\mathrm{Ox}}^{\mathrm{Fc/Fc^+}} + 4.8)(\mathrm{eV}) \quad (1)$$

$$E_{\mathrm{LUMO}} = -e(E_{\mathrm{Red}}^{\mathrm{onset}} - E_{\mathrm{Red}}^{\mathrm{Fc/Fc^+}} + 4.8)(\mathrm{eV}) \quad (2)$$

Table 1 summarizes the Red/Ox properties and energy levels determined from CVA, quantum chemical calculations and UV–vis data. According to the CVA experiments LUMO levels for compounds **4a–c** were estimated in the range −2.83–2.63 eV and for **4d** it was found to be slightly lower (−2.97 eV). HOMO levels were estimated in the range −5.46–5.59 eV for **4a–c** and −5.78 eV for **4d**.

Also, LUMO levels of compounds **4a–d** have been estimated as a sum of HOMO energy (determined from CVA) and the HOMO–LUMO gap (obtained from UV–vis and luminescence spectroscopies). In comparison to electrochemically obtained data these energy levels were a little higher. HOMO levels determined from quantum chemical calculation were in reasonable agreement with the experimental values. The agreement between experimental and calculated LUMO energy levels was poorer, which was probably caused by the small set of basis orbitals used in DFT calculations. It is worth noting that the experimentally obtained HOMO–LUMO gap appeared nearly identical for compounds **4a–c**, and was larger than that of **4d** by about 0.15–0.2 eV, in good agreement with prediction based on DFT calculations.

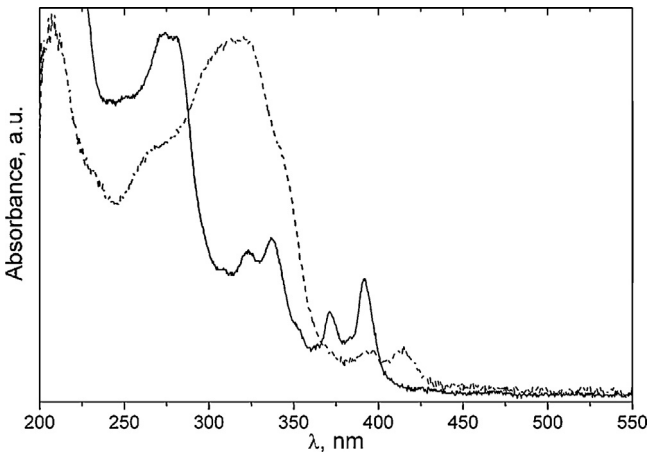

Fig. 3. Normalized UV–vis absorption spectra of thin films of **4b** (solid line) and **4d** (dashed line).

3.4. Light-induced electron transfer

The electron affinity of the semiconducting polymer MEH-PPV, which is often used in organic photovoltaics, is −2.58 eV [24]. According to our CVA measurements, photoinduced electron transfer is allowed from MEH-PPV to the **4d** molecule. Light-induced charge separation in the composite **4d**:MEH-PPV was

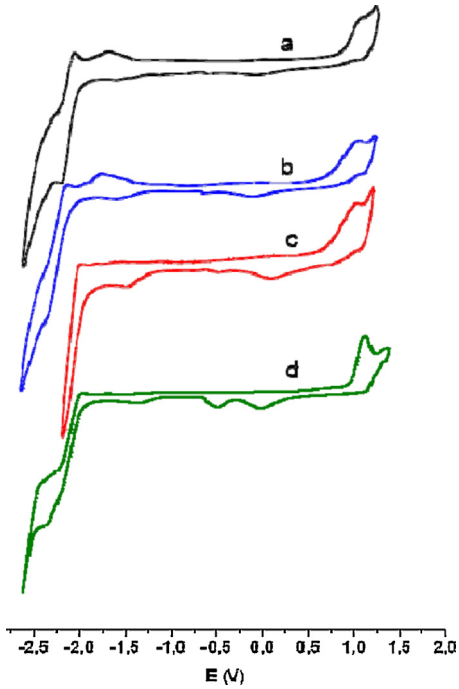

Fig. 4. Cyclic voltammetry plots of compounds **4a–d** measured in 0.1 M $TBAPF_6$ CH_2Cl_2 solution. Potentials calibrated vs. Fc/Fc^+ as an internal standard.

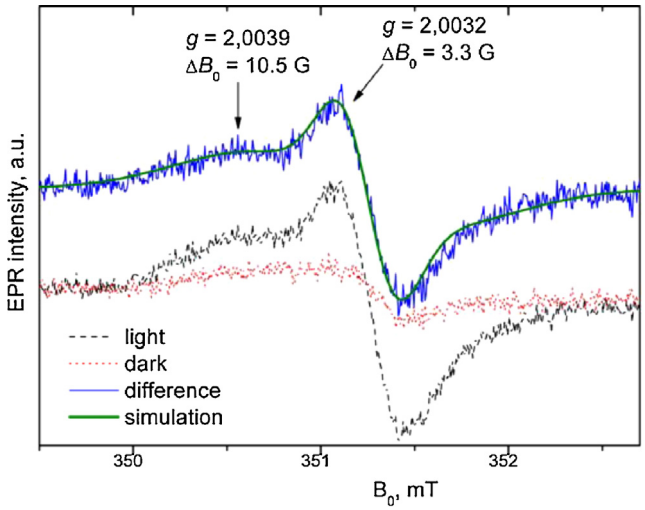

Fig. 5. CW EPR spectra of composite MEH-PPV:**4d** before and under light illumination (dotted and dashed lines, respectively), light-induced EPR spectrum (solid thin line) and its simulation by two Gaussian lines with peak-to-peak widths of 1.05 mT and 0.33 mT (thick line).

observed using the CW EPR technique. Under light illumination, two lines were detected in the EPR spectrum of **4d**:MEH-PPV (see Fig. 5). The narrow EPR line with the width 3.3 G and $g = 2.0032$ was attributed to the MEH-PPV$^+$ cation [25,26]. The broad line with the width of 10.5 G and $g = 2.0039$ was attributed to the **4d**$^-$-anion. We propose that the hyperfine interaction between magnetic nuclei of **4d** backbone and the electron of **4d**$^-$-anion determined this EPR line broadening.

4. Conclusions

2,7-Di(R) naphtho[4,3,2,1-*lmn*][2,9]phenanthrolines **4a**–**d** with R = CH_2OCHMe_2, Hex CH_2OCH_2Ph, Ph were successfully synthesized via heterocyclization between 1,5-diethynyl-9,10-anthraquinones and urea in DMF. The HOMO–LUMO gap for these substances is in the range 2.97–3.16 eV. Light-induced electron transfer from MEH-PPV to **4d** molecules was detected by EPR-spectroscopy. The optical and electrochemical properties of the newly synthesized substances allow us to consider them as possible electron acceptors for organic solar cells, or as building blocks for larger molecules with extended π-conjugated system, which can then be used in organic electronics.

Acknowledgments

This work was supported by the Russian Foundation for Basic Research (grants no. 14-03-31183_mol-a, and no. 15-03-07682a), the Scholarship of the President of the Russian Federation (no. 3596.2013.1), the Ministry of Education and Science of the Russian Federation and the Chemical Service Centre of SB RAS. We wish to thank Stephen Hogg, University of Dundee, United Kingdom, for the helpful proof of this article.

References

[1] C.J. Brabec, V. Dyakonov, J. Parisi, N.S. Sariciftci, Organic Photovoltaics: Concepts and Realization, Springer, Berlin, 2010.
[2] P.A. Troshin, R.N. Lyubovskaya, V.F. Razumov, Nanotechnol. Russ. 3 (2008) 242.
[3] B. Walker, C. Kim, T.-Q. Nguyen, Chem. Mater. 23 (2011) 470.
[4] A. Mishra, P. Bauerle, Angew. Chem. Int. Ed. 51 (2012) 2020.
[5] V.A. Trukhanov, D.Yu. Paraschuk, Polym. Sci. C 56 (2014) 72.
[6] E. Kozma, M. Catellani, Dyes Pigm. 98 (2013) 160.
[7] C. Li, H. Wonneberger, Adv. Mater. 24 (2012) 613.
[8] C.L. Chochos, N. Tagmatarchis, V.G. Gregoriou, RSC Adv. 3 (2013) 7160.
[9] A.V. Mumyatov, L.I. Leshanskaya, D.V. Anokhin, N.N. Dremova, P.A. Troshin, Mendeleev Commun. 24 (2014) 306.
[10] U.H.V. Bunz, J.U. Engelhart, B.D. Lindener, M. Schaffroth, Angew. Chem. Int. Ed. 52 (2013) 3810.
[11] D.S. Baranov, A.G. Popov, M.N. Uvarov, L.V. Kulik, Mendeleev Commun. 24 (2014) 383.
[12] R.W. Higgins, C.M. Suter, J. Am. Chem. Soc. 61 (1939) 2662.
[13] http://www2.sscc.ru/.
[14] J.D.C. Maia, G.A.U. Carvalho, C.P. Mangueira, S.R. Santana, L.A.F. Cabral, G.B. Rocha, J. Chem. Theory Comput. 8 (2012) 3072.
[15] F. Neese, Wiley Interdiscip. Rev. Comput. Mol. Sci. 2 (2012) 73.
[16] A.R. Allouche, J. Comput. Chem. 32 (2011) 174.
[17] D.F. Eaton, Pure Appl. Chem. 60 (1988) 1107.
[18] C.E. Castro, R.D. Stephens, J. Org. Chem. 28 (1963) 2163.
[19] A. Schafer, H. Horn, R. Ahlrichs, J. Chem. Phys. 97 (1992) 2571.
[20] F. Weigend, R. Ahlrichs, Phys. Chem. Chem. Phys. 7 (2005) 3297.
[21] S. Grimme, S. Ehrlich, L. Goerigk, J. Comput. Chem. 32 (2011) 1456.
[22] S. Grimme, J. Antony, S. Ehrlich, H. Krieg, J. Chem. Phys. 132 (2010) 154104.
[23] U. Zvokhaerts, T. Erb, H. Hoppe, G. Gobsch, N.S. Sariciftci, Thin Solid Films 496 (2006) 679.
[24] L.F. Santos, R.C. Faria, L. Gaffo, L.M. Carvalho, R.M. Faria, D. Goncalves, Electrochim. Acta 52 (2007) 4299.
[25] K. Murata, Y. Shimoi, S. Abe, T. Noguchi, T. Ohnishi, Synth. Met. 101 (1999) 353.
[26] S. Kuroda, K. Marumoto, N.C. Greenham, R.H. Friend, Y. Shimoi, S. Abe, Synth. Met. 119 (2001) 655.